Observation of Bimolecular Carrier Recombination Dynamics in Close-Packed Films of Colloidal CdSe Nanocrystals

M. V. Jarosz, N. E. Stott, M. Drndic, N. Y. Morgan, M. A. Kastner, and M. G. Bawendi*

Center for Materials Science and Engineering and Departments of Chemistry and Department of Physics, Massachusetts Institute of Technology, Cambridge, Massachusetts 02139

Received: April 1, 2003; In Final Form: July 23, 2003

We study the intensity dependence of the photoconductivity in close-packed films of CdSe quantum dots in which the photoconductivity is characterized by a low density of trapped charges. We find that the intensity dependence of the photocurrent is nonlinear, which is indicative of bimolecular charge carrier recombination dynamics. We present a physical model for the intensity dependence of the photocurrent that is used to fit the data and extract a ratio of the density of carriers to the density of trapped charges. As our model predicts, we show that the current vs intensity plot becomes more linear when the carrier density is decreased.

Introduction

It has become increasingly apparent that photoionization and charging play an important role in the optical properties of quantum dots (QDs).[1−3] There have been many studies recently probing the electrical properties of semiconductor QDs,[2−14] as well as demonstrations of the application of these electrical properties to devices such as light emitting diodes[15−17] and photovoltaic devices.[18−20] To realize the full potential of semiconductor QDs, and to better comprehend their optoelectronic properties, it is essential to understand the details of their electrical properties. Photoconductivity is a good method for such a study, as it provides information about photoionization, charge transport, and charge carrier recombination.

We present a study of the intensity-dependent photoconduction of close-packed films of CdSe QDs. We show that it is possible to observe photoconduction that is characterized by a low density of trapped charges, in contrast to previous studies. Furthermore, we provide insight into the recombination processes in these films by fitting current vs intensity plots to the steady-state solution of the kinetic equations governing carrier density, which enables us to extract the ratio of carriers to trapped charges. We confirm our physical model of the recombination processes by demonstrating that we can change the shape of the current vs intensity plots as predicted by our model: we can make the plots more linear by decreasing the charge density through decreasing the applied voltage, or by increasing the density of trapped charges through slow aging of the sample.

Experimental Section

Sample Preparation. The quartz substrates used for the photoconductivity measurements are photolithographically patterned with gold electrodes (heights and lengths of 0.11 and 800 μm, respectively). The electrodes used for these experiments are separated by 1 μm, and they are electrically contacted prior to film deposition.

According to the methods of Stott et al.,[21] TOPO/TOP-capped CdSe QDs with a diameter of 47 Å are synthesized by rapid injection of cadmium 2,4-pentanedionate (98%), tri-*n*-octylphosphine (TOP, 90%), 1,2-hexadecanediol (HDDO, 90%), and tri-*n*-octylphosphine selenide (TOPSe, from 1.5 M stock solution) into a hot solvent consisting of TOP, tri-*n*-octylphosphine oxide (TOPO, 99%), and 1-hexadecylamine (HDA, 90%). After the growth solution has cooled to 80 °C, hexane is added to prevent solidification at room temperature. The absorption spectrum after this step for the quantum dots used for these experiments is shown in Figure 1. The solution is then placed in the refrigerator for 1 h and centrifuged to remove excess insoluble organics and any salts that may have formed during the reaction. A precipitation using butanol and hexane as the solvents and methanol as the nonsolvent is repeated three times to remove excess TOPO/TOP which would prohibit close-packing of the QD film.[10,22,23] The precipitations also have the effect of narrowing the size distribution. The hexane/butanol/QD solution is filtered prior to the second and third precipitation using 0.2 μm and 0.1 μm syringe filters, respectively, to further remove excess insoluble organics and salts. According to previously established methods for making close-packed CdSe QD films,[10,23−26] the final precipitate is dried under vacuum and redissolved in a 9:1 mixture of hexane:octane; this solution is filtered through a 0.02 μm syringe filter. The close-packed films are deposited in an inert atmosphere by drop-casting the QD solution on the prepared quartz substrates.[27] Analysis of close-packed regions of QDs in transmission electron microscopy (TEM) images indicates that the QDs are separated by 1.2 ± 0.4 nm, consistent with previous studies.[25] A low-resolution TEM image illustrating the tendency of the QDs to close-pack and a representative high-resolution TEM image confirming the spherical and crystalline nature of the QDs are available in the Supporting Information (Figures 2S and 3S, respectively).

Measurements. The measurement device is shown in the inset of Figure 2. The measurements are performed at 77 K under vacuum in a coldfinger cryostat. The samples are loaded into the cryostat inside of an inert atmosphere glovebox and the cryostat is subsequently evacuated to $<10^{-5}$ Torr so that contact with air is minimized. A Keithley 6517 electrometer is used to measure current as well as to apply a source-drain voltage. The 514 nm line of an Ar^+ laser is used as an excitation source, with excitation intensities up to 25 mW/cm^2. A neutral density filter wheel is used to adjust the excitation intensity for

* Corresponding author.

10.1021/jp034849o CCC: $25.00
Published on Web 10/30/2003

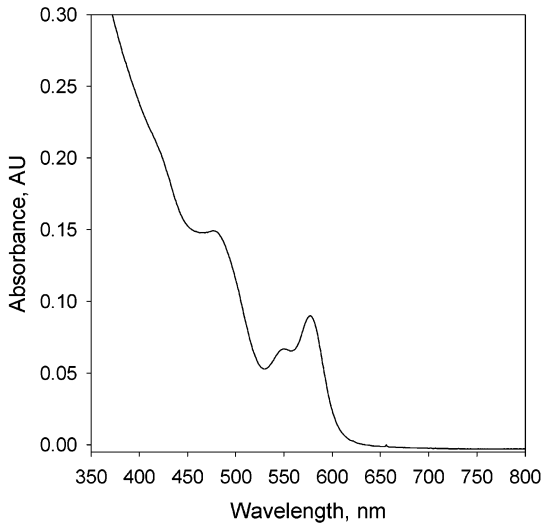

Figure 1. Absorption spectrum of the quantum dots used in these studies.

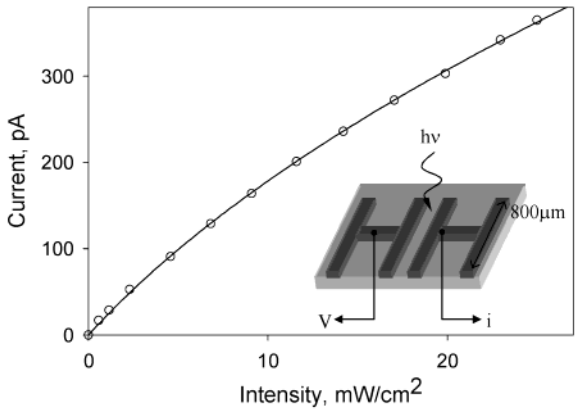

Figure 2. Representative graph of current vs intensity. The circles correspond to the data, and the solid line corresponds to the fit to eq 11. The extracted ratio of n/N_t at the highest measured intensity is ~0.6. The inset shows the measurement device. The substrate is quartz, and the electrodes are 1000 Å of gold on top of 100 Å of titanium. The length of the electrodes is 800 μm, and they are separated by 1 μm. The sample is illuminated with 514 nm light from an Ar^+ laser.

intensity-dependent measurements. Previous work by Leatherdale et al.[10] on the photoconductivity of close-packed films of quantum dots confirms that the photoconduction is field-dependent, that it results from the field-induced separation of excitons, and that it is not due to photoinjection from the gold electrodes.

Results and Discussion

1. Model for Intensity Dependence. We base our physical model for the intensity dependence of the photocurrent on well-established equations for charge carrier kinetics, starting with the equation for the rate of change of the carrier density (n, which is linearly related to the current)

$$\frac{dn}{dt} = G - (N_t + n)nb \tag{1}$$

where G is the rate of photogeneration of carriers and is linearly related to the intensity, N_t is the density of trapped charges, and b is a normalized factor for recombination efficiency.[28] It is assumed that electrons are the majority carrier[10] and that they must recombine with a hole to be removed; the rate of annihilation is represented by the negative term of eq 1. The term $(N_t + n)$ represents the total density of holes available for recombination. There are at least n holes, as each carrier originates from the separation of the electron and hole in the photogenerated exciton. In addition, there are N_t trapped holes in the film that do not have a carrier electron as their counter-charge—that is, for charge neutrality these trapped holes must be associated with an electron that is trapped deep enough that it cannot contribute to conductivity. The most likely scenario is that the trapped holes are in surface-state traps such as unpassivated selenium, and the trapped electrons reside either in the surface ligands (for instance, in an acidic impurity such as those present in TOP) or in radical species such as SeO_2^- or O_2^-.[29] We deduce that SeO_2^- is a likely possibility because it is known that SeO_2 is formed on the surface of oxidized CdSe nanocrystals,[30] and since SeO_2 is often used as an oxidizing agent[31] it is likely that the reduced form, SeO_2^-, could be present on the surface of the nanocrystals.

At equilibrium, the steady-state approximation may be used so that eq 1 becomes

$$G = (N_t + n)nb \tag{2}$$

If the density of trapped charges is much larger than the carrier density, eq 2 reduces to

$$G \approx N_t nb \tag{3}$$

which results in a linear relationship between current and intensity. If, on the other hand, the carrier density is much larger than the density of trapped charges, eq 2 reduces to

$$G = n^2 b \tag{4}$$

which results in the current having a square root dependence on the intensity.

2. Nonlinear Intensity Dependence is Observed. Figure 2 shows a typical graph of current vs intensity. The measurement was taken with an applied field of 10^6 V/cm. As Figure 2 shows, a nonlinear intensity dependence is observed, suggesting that the density of trapped charges in this system is not much larger than the carrier density, and the recombination is best described as bimolecular. This is in contrast to previous work[10] that showed a linear intensity dependence of the photocurrent. The linear intensity dependence was attributed to pseudomonomolecular recombination, meaning that the density of trapped charges is much larger than the carrier density, and thus the recombination is described by eq 3. We suggest that the films we measure here have a lower density of trapped charges, because of the different method used to synthesize the QDs and because the exposure to air has been minimized.

3. Fits to the Data. For further analysis of eq 2, it is necessary to rewrite the equation in terms of the parameters that are measured in the experiment: current (i) and intensity (I). Because the parameters G and n are linearly related to I and i, respectively, we make the following substitutions:

$$Im(V) = G \tag{5}$$

and

$$ia(V) = n \tag{6}$$

where $m(V)$ is a voltage-dependent parameter that incorporates the voltage-dependent exciton separation efficiency and the absorption cross-section of the film. $a(V)$ is a voltage-dependent

parameter, with

$$a(V) = L/(AVe\mu) \tag{7}$$

where L is the length of the electrodes, A is the area of the side of the electrodes in contact with the film, and μ is the mobility. The equation for $a(V)$ is derived from the relationship between conductivity (σ) and n:

$$\sigma = \frac{iL}{AV} = ne\mu \tag{8}$$

These substitutions result in a quadratic equation relating current and intensity (for all values of i and N_t). Because there are only two independent parameters in eq 3, we define

$$\alpha = \left(\frac{b}{m}a^2\right) \tag{9}$$

and

$$\beta = \left(\frac{b}{m}N_t a\right) \tag{10}$$

The intensity dependence of the current then becomes

$$i = \frac{1}{2\alpha}(-\beta + \sqrt{\beta^2 + 4\alpha I}) \tag{11}$$

Equation 11 is used to fit the current vs intensity data, with α and β as the fitting parameters. Figure 2 shows an example of the fit for some representative data.

It is possible with further manipulation of the above equations to extract additional information from the fit parameters. Given eq 6 and that

$$\frac{\alpha}{\beta} = \frac{a}{N_t} \tag{12}$$

it is possible to extract the ratio of carriers to trapped charges at a particular intensity:

$$\frac{n}{N_t} = \frac{\alpha}{\beta}i \tag{13}$$

For the data in Figure 2, $n/N_t \sim 0.6$ at the highest measured intensity value, which confirms that in this case the trap density and the carrier density are of comparable magnitudes.

4. Changing the Shape of *i* vs *I*. Because the deviation from linearity in the i vs I plots depends on the carrier density relative to the density of trapped charges, our model predicts the shape of the curve to have a dependence on voltage. That is, at low voltage (and thus low carrier density), one would expect a more linear response than at high voltage. Figure 3 shows that this behavior is in fact observed. As Table 1 shows, the calculated ratios of n/N_t at fixed intensity follow the expected trend of increasing with voltage, due to the increasing carrier density, n. In addition, the weak dependence of n/N_t on voltage suggests that the exponential dependence of current on voltage is due to the strong voltage dependence of the mobility, rather than n.

In addition to changing the shape of the current vs intensity curve through increasing the carrier density (by increasing the voltage), it should also be possible to change the shape of the curve by increasing the density of trapped charges. Our data suggest that it is possible to do this by slowly aging the sample. With a pressure of only 10^{-5} Torr, there is enough oxygen around that the sample will slowly oxidize if left in the cryostat for an extended period of time. The film was measured on the first day it was loaded in the cryostat (day 1), after remaining in the cryostat for 4 days (day 5), and after remaining in the cryostat for 11 days (day 12). Figure 4 shows the evolution of the shape of the current vs intensity curve at an applied field of 3×10^5 V/cm as the sample is slowly aged. As expected, the curve becomes more linear as the sample ages because the trap density is increased and, as Table 2 shows, the calculated values of n/N_t decrease as well. Counter to our expectations, however, though the curve does become more linear from day 1 to day 5, the current also increases. This increase in current could be due to a mobility increase (perhaps because additional solvent was removed while the sample was at room temperature and

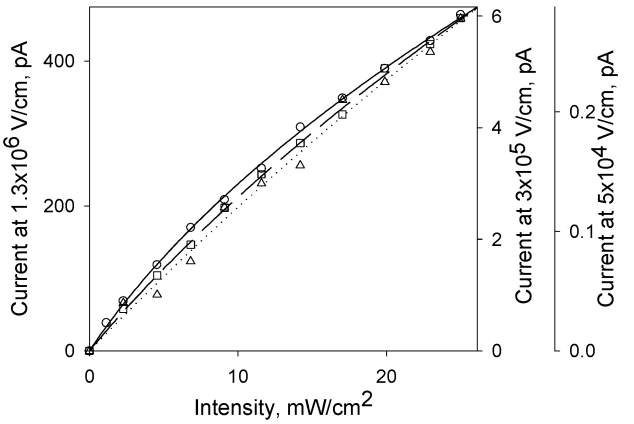

Figure 3. Voltage dependence of the shape of the current vs intensity plot. The circles, squares, and triangles are the data at fields of 1.3×10^6, 3×10^5, and 5×10^4 V/cm, respectively. The solid, dashed, and dotted lines are the fits to eq 11 for the data at 1.3×10^6, 3×10^5, and 5×10^4 V/cm, respectively.

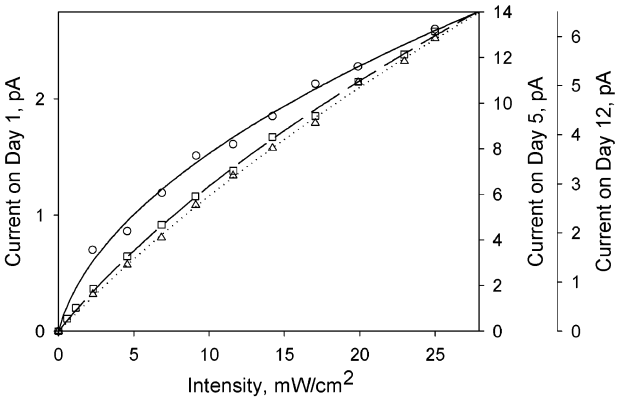

Figure 4. Oxidation dependence of the shape of the current vs intensity plot at a field of 3×10^5 V/cm. The circles, squares, and triangles correspond to the data for day 1, day 5, and day 12, respectively. The solid, dashed, and dotted lines correspond to the fits to eq 2 for the data from day 1, day 5, and day 12, respectively.

TABLE 1: Voltage Dependence of n/N_t at the Highest Measured Intensity for the Data in Figure 3

field, V/cm	n/N_t at highest I
5×10^4	0.17
3×10^5	0.34
1.3×10^6	0.68

TABLE 2: Oxidation Dependence of n/N_t at the Highest Measured Intensity for the Data in Figure 4

day no.	n/N_t at highest I
1	3.8
5	0.58
12	0.34

under vacuum) or an increase in the exciton separation efficiency (perhaps due to residual physisorbed oxygen being removed from the film[32,33]). In the latter case, the increase in n would be accompanied by a even larger increase in N_t (due to aging), therefore still resulting in a decrease in n/N_t.

Conclusion

We present the observation of photoconduction in close-packed films of CdSe quantum dots with a low enough density of trapped charges to exhibit bimolecular carrier recombination. These data are shown to be an improvement over previous measurements, which show quasi-monomolecular recombination dynamics due to having a much higher density of trapped charges than carriers. We attribute the improvement to a different synthetic procedure and the fact that the exposure of the films to air was minimized. The intensity dependence of the photocurrent is fit to an equation that is derived from the equations for carrier recombination dynamics, and the ratio of carrier density to density of trapped charges is extracted. We further confirm that these data are a reflection of the recombination dynamics of the system by demonstrating that we can alter the shape of the current vs intensity curve by changing the carrier density (through changing the voltage), and we suggest that it may also be possible to change the shape by changing the density of trapped charges through slow aging of the sample.

Acknowledgment. We thank the NSF funded MIT Harrison Spectroscopy Laboratory for support and for use of their facilities. This research was supported in part by the Packard Foundation and by the MRSEC program of the National Science Foundation under award number DMR 02-13282 and made use of its shared user facilities. M.V.J. was a Corning fellow and Lester Wolf fellow. We also thank Michael Frongillo for assistance with taking the high-resoltuion TEM images.

Supporting Information Available: Optical micrographs and TEM images. This material is available free of charge via the Internet at http://pubs.acs.org.

References and Notes

(1) Nirmal, M.; Dabbousi, B. O.; Bawendi, M. G.; Macklin, J. J.; Trautman, J. K.; Harris, T. D.; Brus, L. E. *Nature* **1996**, *383*, 802.

(2) Woo, W. K.; Shimizu, K. T.; Jarosz, M. V.; Neuhauser, R. G.; Leatherdale, C. A.; Rubner, M. A.; Bawendi, M. G. *Adv. Mater.* **2002**, *14*, 1068.

(3) Shim, M.; Wang, C.; Guyot-Sionnest, P. *J. Phys. Chem. B* **2001**, *105*, 2369.

(4) Blackburn, J. L.; Ellingson, R. J.; Micic, O. I.; Nozik, A. J. *J. Phys. Chem. B* **2003**, *107*, 102.

(5) Drndic, M.; Jarosz, M. V.; Morgan, N. Y.; Kastner, M. A.; Bawendi, M. G. Submitted to *J. Appl. Phys.*

(6) Ellingson, R. J.; Blackburn, J. L.; Yu, P. R.; Rumbles, G.; Micic, O. I.; Nozik, A. J. *J. Phys. Chem. B* **2002**, *106*, 7758.

(7) Ginger, D. S.; Greenham, N. C. *Phys. Rev. B* **1999**, *59*, 10622.

(8) Ginger, D. S.; Greenham, N. C. *J. Appl. Phys.* **2000**, *87*, 1361.

(9) Ginger, D. S.; Greenham, N. C. *Synth. Met.* **2001**, *124*, 117.

(10) Leatherdale, C. A.; Kagan, C. R.; Morgan, N. Y.; Empedocles, S. A.; Kastner, M. A.; Bawendi, M. G. *Phys. Rev. B* **2000**, *62*, 2669.

(11) Krauss, T. D.; Brus, L. E. *Phys. Rev. Lett.* **1999**, *83*, 4840.

(12) Shim, M.; Guyot-Sionnest, P. *Nature* **2000**, *407*, 981.

(13) Wang, C. J.; Shim, M.; Guyot-Sionnest, P. *Science* **2001**, *291*, 2390.

(14) Wang, C. J.; Shim, M.; Guyot-Sionnest, P. *Appl. Phys. Lett.* **2002**, *80*, 4.

(15) Colvin, V. L.; Schlamp, M. C.; Alivisatos, A. P. *Nature* **1994**, *370*, 354.

(16) Dabbousi, B. O.; Bawendi, M. G.; Onitsuka, O.; Rubner, M. F. *Appl. Phys. Lett.* **1995**, *66*, 1316.

(17) Coe, S.; Woo, W. K.; Bawendi, M. G.; Bulovic, V. *Nature* **2002**, *420*, 800.

(18) Huynh, W. U.; Dittmer, J. J.; Alivisatos, A. P. *Science* **2002**, *295*, 2425.

(19) Huynh, W. U.; Dittmer, J. J.; Teclemariam, N.; Milliron, D. J.; Alivisatos, A. P.; Barnham, K. W. J. *Phys. Rev. B* **2003**, *67*, art. no.

(20) Nozik, A. J. *Physica E* **2002**, *14*, 115.

(21) Bawendi, M. G.; Stott, N. E. U.S. Patent 6,576,291, 2003.

(22) Murray, C. B.; Norris, D. J.; Bawendi, M. G. *J. Am. Chem. Soc.* **1993**, *115*, 8706.

(23) Murray, C. B.; Kagan, C. R.; Bawendi, M. G. *Science* **1995**, *270*, 1335.

(24) Murray, C. B.; Kagan, C. R.; Bawendi, M. G. *Annu. Rev. Mater. Sci.* **2000**, *30*, 545.

(25) Kagan, C. R.; Murray, C. B.; Nirmal, M.; Bawendi, M. G. *Phys. Rev. Lett.* **1996**, *76*, 1517.

(26) Kagan, C. R.; Murray, C. B.; Bawendi, M. G. *Phys. Rev. B* **1996**, *54*, 8633.

(27) These measurements require very rigorous sample preparation to ensure high-quality films. Even with a final filtration step prior to film deposition, filtering once during the size selection causes the photocurrent to go from unmeasurable to measurable. Purifying the TOP adds an additional order of magnitude to the photocurrent, although still produces films that do not look smooth when observed with an optical microscope. If, in addition to these purification steps, the growth solution is put in the refrigerator for 1 h prior to centrifugation and a filtration step is added prior to the second precipitation step as well as the third, one additional order of magnitude is added to the photocurrent, and the films appear smooth when observed with an optical microscope. Optical microscope images of films prepared with different levels of rigor are shown in the Supporting Information, Figure 1S.

(28) Bube, R. H. *Photoconductivity of Solids*; Wiley: New York, 1960.

(29) McNeill, J. D.; Barbara, P. F. *J. Phys. Chem. B* **2002**, *106*, 4632.

(30) Katari, J. E. B.; Colvin, V. L.; Alivisatos, A. P. *J. Phys. Chem.* **1994**, *98*, 4109.

(31) Bagnall, K. W. *The Chemistry of Selenium, Tellurium and Polonium*; Elsevier Publishing Co.: Amsterdam, 1966.

(32) Bube, R. H. *J. Chem. Phys.* **1957**, *27*, 496.

(33) Bube, R. H. *J. Electrochem. Soc.* **1966**, *113*, 793.